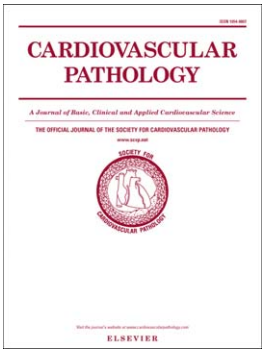

Carbonic Anhydrase Inhibitors Reduce Cardiac Dysfunction after Sustained Coronary Artery Ligation in Rats

Lorena A. Vargas, Oscar A. Pinilla, Romina G. Díaz, Diana E. Sepúlveda, Erik R. Swenson, Néstor G. Pérez, Bernardo V. Álvarez

PII: S1054-8807(16)30093-X
DOI: doi: 10.1016/j.carpath.2016.08.003
Reference: CVP 6938

To appear in: *Cardiovascular Pathology*

Received date: 10 June 2016
Revised date: 15 August 2016
Accepted date: 16 August 2016

Please cite this article as: Vargas Lorena A., Pinilla Oscar A., Díaz Romina G., Sepúlveda Diana E., Swenson Erik R., Pérez Néstor G., Álvarez Bernardo V., Carbonic Anhydrase Inhibitors Reduce Cardiac Dysfunction after Sustained Coronary Artery Ligation in Rats, *Cardiovascular Pathology* (2016), doi: 10.1016/j.carpath.2016.08.003

Carbonic Anhydrase Inhibitors Reduce Cardiac Dysfunction After Sustained Coronary Artery Ligation in Rats

Lorena A. Vargas Ph.D.[a], Oscar A. Pinilla[a], Romina G. Díaz Ph.D.[a], Diana E. Sepúlveda Ph.D.[b], Erik R. Swenson M.D.[c], Néstor G. Pérez Ph.D. [a], and Bernardo V. Álvarez Ph.D. [a*]

[a] Centro de Investigaciones Cardiovasculares, Consejo Nacional de Investigaciones Científicas y Técnicas, Facultad de Ciencias Médicas, Universidad Nacional de La Plata, (1900) La Plata, Buenos Aires, Argentina.

[b] Departamento de Patología, Universidad Favaloro, (C1078AAJ) Ciudad Autónoma de Buenos Aires, Argentina.

[c] Department of Medicine, Pulmonary and Critical Care Medicine, VA Puget Sound Health Care System, University of Washington, Seattle, WA 98108, USA.

[*]**Corresponding author:**

Dr. Bernardo V. Alvarez, Ph.D.
Facultad de Ciencias Médicas
Calle 60 y 120 – (1900) La Plata
Buenos Aires - Argentina
Phone: +54 221 483 4833
Fax: +54 221 483 4833
Email: balvarez@med.unlp.edu.ar

Short Title: Carbonic anhydrase inhibitors and heart failure

Subject Code: Basic Science Research; Animal Models of Human Disease

Abstract

Background- Two potent carbonic anhydrase (CA) inhibitors with widely differing membrane permeability, poorly diffusible benzolamide (BZ) and highly diffusible ethoxzolamide (ETZ) were assessed to determine whether they can reduce cardiac dysfunction in rats subjected to coronary artery ligation (CAL)-induced myocardial infarction.

Methods and results- Rats with evidence of heart failure (HF) at 32 weeks following a permanent left anterior coronary artery occlusion were treated with placebo, BZ or ETZ (4 $mg.kg.day^{-1}$) for 4-weeks at which time left ventricular function and structure were evaluated. Lung weight/body weight (LW/BW) ratio increased in CAL rats by 17±1% vs. control, suggesting pulmonary edema. There was a trend for BZ and ETZ to ameliorate the increase in LW/BW by almost 50% (9±5% and 9±8%, respectively, versus CAL) (*P*=0.16, NS). Echocardiographic assessment showed decreased LV midwall shortening in HF rats, 21±1% vs. control 32±1%, which was improved by BZ to 29±1% and ETZ to 27±1%, and reduced endocardial shortening in HF rats 38±3% vs. control 62±1%, partially restored by BZ and ETZ to ~50%. Expression of the hypoxia-inducible membrane-associated CAIX isoform increased by ~60% in HF rat hearts, and this effect was blocked by ETZ.

Conclusions- We conclude that CAL-induced myocardial interstitial fibrosis and associated decline in left ventricular function were diminished with BZ or ETZ treatment. The reductions in cardiac remodelling in HF with both ETZ and BZ CA inhibitors suggest that inhibition of a membrane-bound CA appears to be the critical site for this protection.

Keywords: heart failure; carbonic anhydrase inhibitors; intracellular pH; myocardial infarction

1. Introduction

Heart failure (HF) remains one of the leading causes of morbidity and mortality worldwide with fibrotic remodeling after myocardial infarction (MI) as the most frequently recognized primary factor [1, 2].

Pathologic cardiac hypertrophy diminishes contractile function and commonly progresses to HF [3]. Changes in ion homeostasis, which result from altered expression and/or function of the ion transporters NHE1 Na^+/H^+ exchanger [4, 5] , AE3 Cl^-/HCO_3^- exchanger [6] and NBC Na^+/HCO_3^- cotransporter [7], and their associated regulatory partners (carbonic anhydrases, CA) [8, 9], contribute to hypertrophic growth. Experimental and clinical studies demonstrate the pathophysiological role of increased NHE1 activity during cardiac ischemia/reperfusion injury and post-injury hypertrophy [10, 11]. The proposed cascade of undesirable events, involving NHE1, AE3, and NBC activation, has been attributed to an increased intracellular Na^+ load [6, 12-14] , and subsequent increase in intracellular Ca^{2+} concentration ($[Ca^{2+}]_i$). Augmented $[Ca^{2+}]_i$ then triggers widely-recognized Ca^{2+}-dependent intracellular signaling pathways leading to cardiac hypertrophy [15-18].

Interestingly, we have identified a role for CA in the hypertrophic growth of cultured cardiomyocytes exposed to phenylephrine (PE), angiotensin II (AngII), or endothelin 1 (ET1) [8]. Treatment of hypertrophically-stimulated cardiomyocytes with the freely diffusible potent CA inhibitor, ethoxzolamide (Cardrase, ETZ) diminished the hormonally-induced hypertrophy and reversed it after once established. These effects appear to involve enhanced intracellular Na^+ and Ca^{2+} loading [8]. Furthermore, cultured myocytes of CAII-deficient mice did not respond to the same pro-hypertrophic stimulation, suggesting a role of CAII in promoting cardiac hypertrophy [19].

We recently reported that failing human hearts (of ischemic and non-ischemic origin) in non-diabetic patients are characterized by increased CAII and CAIV expression [9]. Moreover, myocardial CA activation was found to be present in human diabetic ischemic cardiomyopathy (HDIC) [20]. Indeed, CAI and CAII isozymes are overexpressed in HDIC, and the increased myocyte expression of CAII is associated with the NHE1 Na^+/H^+ exchanger hyperphosphorylation in this specific diabetic HF condition [20]. Therefore, on the basis of these findings it is tempting to speculate that CA inhibition with existing drugs could be rapidly implemented and would be therapeutic for diabetic patients with post-MI HF. Because CA overexpression is identified as a marker of the hypertrophic human heart that progresses towards failure [9], CA inhibition might be an appropriate strategy to moderate the hypertrophic cascade.

The CAIX isozyme is expressed in the mammalian heart [21], localizing to the t-tubules of cardiomyocytes [22]. CAIX, whose gene has a hypoxia inducible factor (HIF) responsive element in its promoter region, is overexpressed in hypoxic tumors and is essential in promoting tumor growth and metastasis [23, 24]. However, CAIX expression is not limited to cancer, but may be also induced in other pathological situations associated with ischemia, fibrosis, vascular remodeling, inflammation or metabolic disturbances such as heart failure that lead to activation of the HIF pathway. In the setting of heart failure changes in mitochondrial metabolism lead to possibly injurious reactive oxygen species (ROS) generation and a greater reliance of glycolytic metabolism [25]. CAVB isozyme is a mitochondrial CA involved in cellular metabolism [26] and could be altered in the failing heart.

The functional benefit of CA inhibition has not been evaluated in cardiac dysfunction after experimental MI. In the present study we examined the effect of CA inhibitors on rat heart function and collagen deposition following MI and subsequent pathological hypertrophic remodeling, induced by left anterior descending coronary artery ligation (CAL), and we

investigated a potential link of CAIX and CAVB with the development of heart failure following myocardial infarction.

2. Methods

Protocols that involved rats were submitted to, reviewed and approved by the Animal Welfare Committee of La Plata School of Medicine and performed in accordance with the Guide for the Care and Use of Laboratory Animals (Argentine Republic Law N° 14346), concerning animal protection.

2.1. Animals

A total of 52 three-month old male Wistar rats, originally derived from Charles River Breeding Farms (Wilmington, Mass) were used in these studies. All animals were housed under identical conditions and had free access to standard dry meal and water.

2.2. Experimental protocol and group assignments

Myocardial infarction (MI) was produced in 16 three-month old Wistar rats by permanent ligation of the left anterior descending (LAD) coronary artery, according to a method previously described [27]. Thirty six age-matched rats that did not undergo CAL were maintained under identical housing conditions and served as controls. Briefly, the 16 rats subjected to surgery were fully anesthetized by an i.p. injection of Euthanyl (sodium pentobarbital, 35 $mg.kg^{-1}$) and then quickly intubated and ventilated with ambient air using a positive-pressure respirator (Model 680, Harvard). A left thoracotomy was performed via the fourth intercostal space, and the lungs retracted to expose the heart. The LAD coronary artery was ligated with a 7-0 silk suture near its origin. Acute ischemia was deemed successful when the anterior wall of the left ventricle became cyanotic. Atelectatic lung regions near the heart were re-inflated by increasing positive end-expiratory pressure, and the thoracotomy site was closed in layers. The animals were then allowed to recover from anesthesia and separated into three experimental groups. All animals

survived the surgery and the myocardial infarction and none died before reaching the time of pre-planned terminal measurements either at 3 or 36 weeks. Similar observation of survival and degree of MI achieved by CAL in rats has been reported before [27, 28]. Table 1 provides detailed information about group assignments, the number of animals used, the treatments given, and the measurements made in each group. The condition of the animals was monitored on a daily basis. Four rats subjected to CAL-induced MI were used only to determine the infarct size and degree of myocardial damage attained at 3 weeks post MI and to assess echocardiographic estimates of LV function at 1 and 3 weeks post MI. These rats were euthanized at three weeks later and the heart was removed for histological studies. All of these parameters obtained at 3 weeks post MI in this group were used for comparison with the functional and histological status of the hearts of the remaining animals subjected to CAL and maintained for 36 weeks.

2.3. Carbonic anhydrase inhibitors treatment in rats subjected to sustained CAL

Of the 12 rats with CAL and taken out to 36 weeks, 6 had no treatment. Three of these only had pathological examination and the other three additionally had echocardiography and immunoblotting for CA VB and CAIX (described below). The remaining six were either treated with the potent freely diffusible CA inhibitor ethoxzolamide (6-Ethoxy-1, 3-benzothiazole-2-sulfonamide; ETZ) (n= 3) or the poorly membrane-permeable potent CA inhibitor, benzolamide ((5-(benzenesulfonamido)-1, 3, 4-thiadiazole 2 sulfonamide; BZ)) (n= 3) [29, 30].

The structures of the two drugs are given below.

Ethoxzolamide

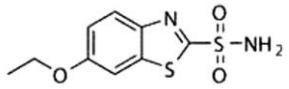

Benzolamide

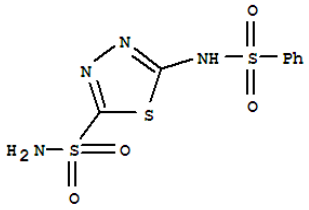

2.4. Echocardiographic examination

Rats were studied echocardiographically under light anesthesia (35 mg.kg^{-1} Euthanyl IP) by two-dimensional M-mode echocardiography with a 7-MHz transducer at the beginning and at the end of protocol. Measurements were performed according to the American Society of Echocardiography leading-edge method [31].

Functional midwall shortening (MS) and endocardial fractional shortening (EFS) were calculated as follow:

$$MS\ (\%) = \frac{[LVDD + ((IVSDTh + PWDTh)/2)] - [LVSD + ((IVSSTh + PWSTh)/2] *100}{[LVDD + ((IVSDTh + PWDTh)/2)]}$$

$$EFS\ (\%) = \frac{(LVDD - LVSD) *100}{LVDD}$$

2.5. Pathologic studies

At the end of the study, body weight was determined and the animals were euthanized under ether anesthesia. The hearts were removed and trimmed of pericardium, fat and blood vessels. The atria were removed and the right and left ventricles were weighed on an analytical balance.

Whole heart weight/tibia length (HW/TL) ratio ($mg.mm^{-1}$) was measured as indicator of cardiac hypertrophy. Lungs were carefully separated and patted dry before weighing.

2.6. Measurements of infarct size

The hearts were immersed in 10% buffered formaldehyde for 48 h and sectioned transversally to the main axis and embedded in paraffin. Three μm tissue sections were stained with hematoxylin-eosin and trichrome. Scar size and infarcted wall thickness were determined on Masson´s trichrome stained sections with a morphometric analysis system (Image ProPlus 4.5, Media Cybernetics, Rockville, MD, USA).

2.7. Histological analysis of collagen deposition

For interstitial fibrosis determination, 3- to 4-μm thick -sections of each heart were cut from apex to base and the left ventricles evaluated for collagen deposition. The tissue slides were processed for paraffin embedding and stained with Masson's trichrome. Sections were imaged at 40x, 200x, and 400x magnification by bright field microscope (LX71 Olympus, Tokyo, Japan). The percentage of collagen was calculated as the sum of collagen areas divided by the total LV area (myocytes + collagen).

2.8. Immunoblot analysis

At the end of the experimental protocol, rat heart samples were harvested and ventricles dissected out. Tissue was disrupted in PBS Buffer (140 mM NaCl, 3 mM KCl, 6.5 mM Na_2HPO_4, 1.5 mM KH_2PO_4, pH 7.5), containing protease inhibitors (PI, MiniComplete Tablet, Roche). After disruption, ventricular lysates were prepared by addition of SDS-PAGE sample buffer, heated at 70 °C, 3 min, and centrifuged 10 min at 16,110 x g. Protein was quantified and 100 μg of protein subjected to 12% SDS-PAGE. Protein samples were transferred to PVDF membranes and then

incubated with mouse anti-CAIX (M75) monoclonal antibody (1:3000 dilution), which recognize the proteoglycan-like attachment domain of CAIX [32], goat anti-CAVB antibody (goat polyclonal R-20; Santa Cruz Biotechnology; 1:500), or mouse anti-gliceraldehyde 3-phosphate dehydrogenase (GAPDH) antibody (1:1000 dilution). Immunoblots were then incubated with donkey anti-mouse conjugated to horseradish peroxidase (HRP) (1:2000), or donkey anti-goat conjugated to HRP (GE Healthcare, Little Chalfont, UK; 1:2000), as appropriate. Blots were visualized and quantified using ECL reagent and a Bio-Rad Image Station.

2.9. Design and statistical analysis

As experiments were performed on rats of similar age and identical genetic and domestic background, data from individual experiments and observations (images of left ventricle sections demonstrating collagen deposition, Figure 5) were pooled for statistical analysis. The number of experiments as a basis for statistical analysis is shown in the figures. Experiments were carried out in a double-blind fashion. Data were compared using Student's t-test when control group and CAL group were compared before treatment, or Kruskal-Wallis Nonparametric ANOVA test followed by the Dunn´s Multiple Comparisons post hoc test for multiple comparisons when an overall significance was established, and when control, CAL, and CAL+ETZ, and CAL+BZ, groups where compared after treatment. GraphPad InStat TM Software was used for statistical analysis. Data are expressed as mean ± SEM. $P < 0.05$ was considered a threshold for statistical significance.

3. Results

3.1. Effect of sustained left coronary artery ligation

The scar size and infarct wall thickness were determined by Masson trichrome staining (Fig. 1). Morphometric analysis of hearts measured in 3-month old Wistar rats not subjected to CA inhibitor treatments showed that the CAL surgical procedure provoked a mean infarct size at 3 weeks post CAL of 21±1% (Fig. 1B, n= 4) consisting of collagen scar tissue replacement of normal tissue (Fig. 1A), and infarct wall thinning (1C, n= 4), which is in agreement with previous observations [27]. In addition, echocardiographic recordings performed in rats exposed to MI demonstrated a significant reduction in the left ventricular endocardial shortening function (~70% relative to control) compared to data obtained in same animals before the MI occurred (n= 4,) (Fig. 1D). Thus, the data demonstrate that CAL-induced MI changed cardiac morphology and function 3 weeks after the procedure and would predict further deterioration with longer follow-up.

Myocardial infarction was produced in rats by CAL and maintained for a total of 36 weeks. A group of non-infarcted rats were maintained for 36 weeks and used as control group. At 32 weeks, CAL rats were kept up to additional 4 weeks without treatment, or were treated with the freely diffusible CA inhibitor, ETZ, or the poorly membrane-permeable CA inhibitor, BZ. Thirty two weeks after ligation, the hearts of infarcted rats had a slightly increase in the left ventricular systolic diameter (LVSD), and left ventricular diastolic diameter (LVDD) (Fig. 2 and Table 1). In addition, the infarcted hearts showed a reduction in the interventricular systolic thickness, compared to control (Table 2). The posterior wall systolic thickness was also reduced in infarcted animals versus control (Table 2).

A modest increase in HW/TL ($mg.mm^{-1}$) ratio of 24±0.4 in CAL vs. 21±0.4 in controls was detected at the end of the study (36 weeks after CAL), which suggests that the ischemic insult promoted moderate myocardial hypertrophy in the surviving ventricular zone (*not shown*). No significant difference in heart rate between the experimental rat groups was observed during the treatment (*not shown*).

3.2. Effect of CA inhibition on heart function and cardiac parameters, after sustained left coronary artery ligation

With the aim of establishing a dose capable of improving evidence of heart dysfunction after CAL-induced MI in rats, in a pilot study we treated 4-month old spontaneously hypertensive rats (SHR) with ETZ 4 $mg.kg^{-1}.day^{-1}$ for 4 weeks and the systolic blood pressure (SBP) was evaluated by the plethysmographic tail-cuff method. The SBP did not change in control SHR after 4 weeks (190±2 mmHg vs. 188±1 mmHg, n= 4), however, ETZ significantly reduced SBP in SHR after 4 weeks (188±2 mm Hg vs. 167±1 mm Hg, before and after treatment, respectively (n= 4, *data not shown*). Having found a dose yielding a possibly relevant cardiovascular effect we chose 4 $mg.kg^{-1}.day^{-1}$ of ETZ or BZ for treatment of rats after prolonged MI.

As mentioned above, LVSD was increased in infarcted hearts at 32 weeks (Table 2, Fig. 2B), and worsened (became greater) over the next four more weeks (Fig. 2A, 2B). At this stage, LVDD also progressed modestly to increase the chamber size at end-diastole (Fig. 2C). In addition, the lung weight/body weight ratio (LW/BW, $mg.g^{-1}$) increased significantly in CAL rats, suggestive of pulmonary edema and a transition to HF (Fig. 3). These architectural rearrangements of the wall and chamber in CAL rats were accompanied by decreased midwall shortening and decreased endocardial fractional shortening of the left ventricle (Fig. 4).

The CA inhibitors ETZ (slightly) and BZ (significantly) decreased the augmented LVSD found in infarcted rat hearts (Fig. 2A, 2B). Interestingly, ETZ and BZ reduced the augmented LVDD in CAL rats to control levels and even further (Fig. 2C). In support of these above indices and a reduction in lung water accumulation as a consequence of heart failure, there was a trend for BZ and ETZ to ameliorate the increase in LW/BW observed in CAL rats (~17%) by almost 50% (9±5% and 9±8%, respectively), but this did not reach statistical significance (P= 0.16) (Fig. 3). Left ventricular function estimated by midwall shortening (Fig. 4A and 4B) and endocardial shortening (ES) (Fig. 4C and 4D), was significantly reduced in CAL rats after prolonged MI, to approximately 60% relative to control (Fig. 4B and 4D, respectively). ETZ and BZ improved the heart function of rats subjected to CAL measured echocardiographically by MS and ES (Fig. 4A-D).

3.3. CA inhibition and cardiac fibrosis after sustained left coronary artery ligation

Cardiac fibroblasts, which rapidly proliferate following Ml, are primarily responsible for the deposition of extracellular matrix (ECM). ECM deposition in infarcted hearts was assessed, using Masson's trichrome staining of histological sections of the hearts (Fig. 5A). The interstitial fibrotic area of CAL rats increased significantly compared with control animals (1.9±0.4% for control vs. 7.5±1.1% for CAL) (Fig. 5A, 5B). Treatment with ETZ reduced ECM deposition by roughly 50%, with a fibrotic area of 3.9±0.8%. Equally, BZ also significantly reduced cardiac collagen deposition 3.4±0.8% (Fig. 5B), proving as well the efficacy of a poorly-membrane diffusive CA inhibitor on cardiac remodeling after acute MI. Thus, CAL induced an increase in interstitial fibrosis, which was reversed by 4-weeks of BZ and ETZ therapy.

3.4. Altered CAIX protein expression in failing hearts

Similar to the increase expression of CAIX protein in hearts of rats subjected to chronic hypoxic conditions [33] and in cultured cardiomyocytes exposed to physiological or chemical hypoxia [34], we found that whole heart lysates obtained from hearts after the experimental protocol revealed the expression levels of CAIX after prolonged CAL-induced MI and heart failure, and after ETZ and BZ treatments.

Whole heart lysates obtained from harvested hearts after experimental protocol were used to quantified CA expression. Herein, immunoblots revealed the expression levels of CAIX which might be altered upon prolonged CAL-induced MI and heart failure, and after ETZ and BZ treatments, in adult rats (Fig. 6A). Expression was quantified by densitometry of the immunoblots and values were corrected for loading differences by normalization to GAPDH levels. CAIX expression was significantly increased with CAL-induced heart failure, but this response was blunted by the CA inhibitor, ETZ in CAL-rats (Fig. 6B). Furthermore, the potent CA inhibitor with reduce membrane permeability, BZ, prevented the increase in CAIX expression elicited by CAL (Fig. 6B). Conversely, expression of CAVB protein (a mitochondrial CA) did not change after CAL (Fig. 6C).

4. Discussion

In this study, we examined two CA inhibitors with broadly different membrane permeability, ETZ and BZ, on heart function and histology in rats subjected to permanent CAL. Our major findings are: 1) Both ETZ and BZ showed a trend towards reduction of pulmonary edema; 2) BZ reduced the modest increase in LV diastolic dimension in CAL-infarcted rats and ETZ and BZ decreased the extent of LV systolic diameter enlargement in infarcted rat hearts; 3) ETZ and BZ minimized the decrease in left ventricular midwall shortening, and left ventricular endocardial shortening (to some extent) observed in HF as measured by echocardiography; 4) BZ and ETZ reversed the interstitial fibrotic remodeling of the heart long following CAL; and 5) the hypoxia inducible isoform of CA, CAIX, which increases after sustained CAL-induced MI, might be involved in the pathophysiological response of the failing heart caused by CAL.

Heart failure is a particularly difficult problem and no single drug or drug class is capable of providing complete symptomatic relief or halting deterioration. Clinically, the standard loop diuretics have clear benefits in congestive heart failure (CHF) and remain the most potent drugs available to relieve symptoms and treat edema [35]. Historically, the membrane permeant CA inhibitor ACTZ was the first oral diuretic used severe CHF [36], but it and other CA inhibitors such as ETZ are very much weaker diuretics and may only reduce body weight by 1-2% [36]. CA inhibitors were soon supplanted by the more potent loop diuretics and other diuretics acting more distally in the nephron [37]. Presently, CA inhibitors are used in CHF mainly to offset the metabolic alkalosis that often develops with chronic use of loop diuretics.

Despite their limited use as first line management of CHF for the past several decades, CA inhibitors have not been examined for actions beyond their diuretic effect as extensively as other drugs used in HF, such as beta blockers, mineralocorticoid antagonists, and afterload

reducing (vasodilating) agents. However, given the fact that there is CA in the myocardium, there may be other salutary effects of CA inhibition [38].

Critical hemodynamic changes in HF arise from ventricular remodeling, which is common with chronic dysfunction of the heart, and they vary with the cause of HF [39]. ECM remodeling, a determinant of ventricular morphology, occurs with development of fibrosis following MI and is a marker of early necrosis [40]. If not prevented, this can lead to thinning of the ventricular wall and further impairment of pump function. Here we observed that increases in systolic and diastolic left ventricle chamber dimensions with reduced ventricular function after sustained CAL-induced infarction in adult rats could be attenuated by treatment with two different CA inhibitors. The equivalence and perhaps even slight superiority of BZ over ETZ, suggests that the critical site of CA inhibition is on the extracellular domain, where several membrane bound CA isoforms may assemble intimately with trans-membrane ion exchangers, such as NHE1, AE3 and NBC transporters [8, 22, 41]. We have earlier shown that CA acts to supply critical H^+ or HCO_3^- to these exchangers that then cause intracellular alkalization and hypertrophic signaling [42].

CA II, CA IV, and CAXIV are increased in ventricles of hypertrophic or failing rat and human hearts [9, 41]. However, expression of CAIX and CAVB has not been explored in these pathological conditions. The *CAIX* gene is under control of the hypoxia-inducible transcription factor (HIF-I) [24]. In addition, hypoxia induced- increases in another HIF (HIF-2α) stimulate miR-210 and CAIX expression, both of which drive fibroblast proliferation in idiopathic pulmonary fibrosis (IPF) [43]. Silencing HIF-2α inhibits the hypoxia-mediated increase in miR-210 expression and blocks IPF fibroblast proliferation. We suggest that inhibition of cardiac fibrosis in the failing hearts of rat subjected to CAL could be possibly due to inhibition of hypoxia-inducible CAIX expression and/or function. However, this hypothesis needs further

examination using selective CAIX inhibitors, genetic knockdown or knockout manipulations. Lastly, we found no changes on the expression of the metabolically-linked mitochondrial CAVB in the hearts of HF rats suggesting that CAVB activity is not involved in the pathological remodeling of the infarcted heart, and seems to be irrelevant in the context of the experiments performed herein. However, studies with specific inhibitors of this isozyme would be much more informative in elucidating its role in the pathologic heart.

Previously, we demonstrated that CA works with the AE3 Cl^-/HCO_3^- exchanger and NHE1 Na^+/H^+ exchanger to promote cardiac hypertrophy [8], as is found in heart failure. Carbonic anhydrases catalytically produce HCO_3^- and H^+ for efflux by AE3, and NHE1, respectively. In addition, NBC Na^+/HCO_3^- cotransporter couples to carbonic anhydrases, which provides the HCO_3^- substrate, maximizing the activity of the transporter [44]. AE3 and NHE1 activity promote hypertrophy and increases in expression of the CA enzymes in cultured rat cardiomyocytes [8]. Sustained NHE1/AE3/NBC activation is itself pro-hypertrophic as the elevation of $[Na^+]_i$ promoted by these transporter could in turn activate the reverse mode of the Na^+/Ca^{2+} exchanger, catalyzing an increase in the cytosolic Ca^{2+} levels. Elevated Ca^{2+} is a consummate hypertrophic signal, working through the calcineurin/NFAT signaling cascade. Recently, it was demonstrated that AE3 gene deletion prevents cardiomyocyte hypertrophy and reduces the rate of pHi recovery in cardiomyocytes, reinforcing the importance of AE3 in cardiovascular pH regulation and the development of cardiomyocyte hypertrophy [45]. To interfere with the hypertrophic cascade present in heart failure we propose that CAs represent targets for anti-hypertrophic therapy. The membrane permeant CA inhibitor, ETZ, which targets the CA-AE3, CA-NHE1, and likely the CA-NBC, complexes, intervenes in the feed-forward cascade, preventing and reversing agonist-induced cardiomyocyte growth [8]. Interestingly,

cardiomyocytes from CAII-deficient mice do not respond to prohypertrophic stimulation, supporting a role of CAII in promoting cardiac hypertrophy [19].

Several stressors as a consequence of MI such as sympathetic activation, pro-hypertrophic factors, cardiac muscle over-stretch, linked hyperactivity of NHE1 and subsequent Ca^{2+} overload lead to cardiac hypertrophy [*for review, see Cingolani* [46]]. Likewise, some of these same factors promote increased CA expression with concomitant Ca^{2+} disturbance as observed in experimental models [8, 19], as well as in human hypertrophic and failing hearts [9]. By inhibiting CA and slowing the rate and magnitude at which the membrane NHE1 alkalinizes the cell, activates Ca^{2+} signaling [47] and initiates hypertrophy [48, 49] ETZ or other CA inhibitors may be therapeutic in limiting catecholamine-driven remodeling and detrimental hypertrophy, major causes of heart failure development [8, 19]. Figure 7 provides a schematic representation of these critical factors and events.

We have shown that chronic treatment with two different CA inhibitors reduces myocardial fibrosis in a rat model of chronic LAD occlusion and improves LV function compared to control. In a similar fashion, CA activation in the hearts of diabetic patients is detectable and associated with increased NHE1 expression and myocyte hypertrophy [20]. Furthermore, in a model of ischemia-reperfusion injury in the rat heart we have preliminary evidence that ETZ reduces total infarct volume and lessens the decline in LV ejection fraction (*Alvarez et al, in submission*). The expression of CAIX as we have shown in the hypoxic and ischemic myocardium is a hypoxia inducible factor (HIF) responsive gene also expressed in cancers and is growth-promoting. Selective inhibition of this isozyme might be useful when specific CA IX inhibitors, now in phase 3 clinical studies, become available.

Our study has several limitations that warrant discussion. The first was the effect of CA inhibitors modulating blood pressure, in rats treated with ETZ and BZ by a month. It is

conceivable that the benefits we observed may have been in part due to reduced afterload, such as found with other drugs having arterial vasodilating properties. While CA inhibitors have not been generally useful as vasodilators by acting directly on vascular smooth muscle CA isoenzymes [37], this possibility cannot be ruled out.

Diuretics reduce peripheral and pulmonary edema in CHF and the reductions in LW/BW ratios with ETZ and BZ (Fig. 3) are consistent with a reduction in lung edema or a greater fractional reduction in lung water than that of total body water. However, in the case of BZ, body weights with treatment after CAL were no different than the untreated controls (Table 2), suggesting little if any important diuretic effect. The ETZ group in contrast was somewhat heavier than controls (Table 3), so the reduction in the LW/BW ratio with both drugs points much more strongly to improved cardiac function rather than any significant diuretic effect. Ideally the use of an equally mild non-CA inhibiting diuretic would have served as a better control for any effect of diuresis.

The other possibility we did not control for is the likely metabolic acidosis that all CA inhibitors cause from their action in the kidney to cause bicarbonate losses. We do not think that the benefits we found could be explained by metabolic acidosis, because an acidotic state usually evokes increased sympathetic activity [50], which itself places a burden on the injured heart and may lead to hypertrophy and fibrosis [51].

5. Conclusions

In a rat model of prolonged MI, CA inhibition by BZ and ETZ initiated in a context of established HF improves cardiac function, limits interstitial fibrosis and prevents LV remodeling, suggesting that CA blockade might be a therapeutic option in the treatment of HF, particularly if cardiac-specific CA inhibitors could be developed. By virtue of their differences in intracellular

penetration, the inhibition of membrane bound CA isozymes, in particular CAIX (BZ and ETZ), rather than intracellular cytosolic isozymes (ETZ only) appears to be the critical site of CA inhibition in the reduction of post infarction cardiac dysfunction and fibrotic remodeling. Thus, CA inhibition with existing and newly optimized drugs could be quickly implemented to: 1) inhibit the CA enzymes whose activity and expression increase as hypertrophy worsens; and 2) prevent the overt activation of membrane transporters (primarily NHE1, but also NBC, and AE3 transporters) involved in pathologic cardiac conditions.

Acknowledgments

BVA and NGP are Established Investigators of the Consejo Nacional de Investigaciones Científicas y Técnicas (CONICET, Argentina). We thank Dr. Joseph Casey (University of Alberta, Canada) for his comments on the manuscript. This work was funded by a Grant from Agencia Nacional de Promoción Científica y Tecnológica to BVA (FONCyT, PICT2013 N° 1976). LAV was a recipient of a felloship from Consejo Nacional de Investigaciones Científicas y Técnicas (CONICET, Type II Postdoctoral Felloship).

Disclosures

None.

References

[1] Pfeffer MA, Braunwald E. Ventricular remodeling after myocardial infarction. Experimental observations and clinical implications. Circulation. 1990;81:1161-72.

[2] Pfeffer MA. Left ventricular remodeling after acute myocardial infarction. Annu Rev Med. 1995;46:455-66.

[3] Frey N, Olson EN. Cardiac hypertrophy: the good, the bad, and the ugly. Annu Rev Physiol. 2003;65:45-79.

[4] Karmazyn M, Gan XT, Humphreys RA, Yoshida H, Kusumoto K. The myocardial Na^+-H^+ exchange: structure, regulation, and its role in heart disease. Circ Res. 1999;85:777-86.

[5] Nakamura TY, Iwata Y, Arai Y, Komamura K, Wakabayashi S. Activation of Na^+/H^+ exchanger 1 is sufficient to generate Ca^{2+} signals that induce cardiac hypertrophy and heart failure. Circ Res. 2008;103:891-9.

[6] Perez NG, Alvarez BV, Camilion de Hurtado MC, Cingolani HE. pH_i regulation in myocardium of the spontaneously hypertensive rat. Compensated enhanced activity of the Na^+-H^+ exchanger. Circ Res. 1995;77:1192-200.

[7] Yamamoto T, Shirayama T, Sakatani T, Takahashi T, Tanaka H, Takamatsu T, et al. Enhanced activity of ventricular Na^+-HCO_3^- cotransport in pressure overload hypertrophy. Am J Physiol. 2007;293:H1254-64.

[8] Alvarez BV, Johnson DE, Sowah D, Soliman D, Light PE, Xia Y, et al. Carbonic anhydrase inhibition prevents and reverts cardiomyocyte hypertrophy. J Physiol. 2007;579:127-45.

[9] Alvarez BV, Quon AL, Mullen J, Casey JR. Quantification of carbonic anhydrase gene expression in ventricle of hypertrophic and failing human heart. BMC Cardiovasc Disord. 2013;13:2.

[10] Yoshida H, Karmazyn M. Na^+/H^+ exchange inhibition attenuates hypertrophy and heart failure in 1-wk postinfarction rat myocardium. Am J Physiol Heart Circ Physiol. 2000;278:H300-4.

[11] Karmazyn M. Mechanisms of protection of the ischemic and reperfused myocardium by sodium-hydrogen exchange inhibition. J Thromb Thrombolysis. 1999;8:33-8.

[12] Camilion de Hurtado MC, Alvarez BV, Perez NG, Ennis IL, Cingolani HE. Angiotensin II activates Na^+-independent Cl^--HCO_3^- exchange in ventricular myocardium. Circ Res. 1998;82:473-81.

[13] Baartscheer A, Schumacher CA, van Borren MM, Belterman CN, Coronel R, Fiolet JW. Increased Na^+/H^+-exchange activity is the cause of increased $[Na^+]i$ and underlies disturbed calcium handling in the rabbit pressure and volume overload heart failure model. Cardiovasc Res. 2003;57:1015-24.

[14] Baartscheer A, Hardziyenka M, Schumacher CA, Belterman CN, van Borren MM, Verkerk AO, et al. Chronic inhibition of the Na^+/H^+ - exchanger causes regression of hypertrophy, heart failure, and ionic and electrophysiological remodelling. Br J Pharmacol. 2008;154:1266-75.

[15] Balke CW, Shorofsky SR. Alterations in calcium handling in cardiac hypertrophy and heart failure. Cardiovasc Res. 1998;37:290-9.

[16] Wilkins BJ, Molkentin JD. Calcium-calcineurin signaling in the regulation of cardiac hypertrophy. Biochem Biophys Res Commun. 2004;322:1178-91.

[17] Wilkins BJ, Dai YS, Bueno OF, Parsons SA, Xu J, Plank DM, et al. Calcineurin/NFAT coupling participates in pathological, but not physiological, cardiac hypertrophy. Circ Res. 2004;94:110-8.

[18] Marks AR. Arrhythmias of the heart: beyond ion channels. Nat Med. 2003;9:263-4.

[19] Brown BF, Quon A, Dyck JR, Casey JR. Carbonic anhydrase II promotes cardiomyocyte hypertrophy. Can J Physiol Pharmacol. 2012;90:1599-610.

[20] Torella D, Ellison GM, Torella M, Vicinanza C, Aquila I, Iaconetti C, et al. Carbonic anhydrase activation is associated with worsened pathological remodeling in human ischemic diabetic cardiomyopathy. J Am Heart Assoc. 2014;3:e000434.

[21] Scheibe RJ, Gros G, Parkkila S, Waheed A, Grubb JH, Shah GN, et al. Expression of membrane-bound carbonic anhydrases IV, IX, and XIV in the mouse heart. J Histochem Cytochem. 2006;54:1379-91.

[22] Orlowski A, De Giusti VC, Morgan PE, Aiello EA, Alvarez BV. Binding of carbonic anhydrase IX to extracellular loop 4 of the NBCe1 Na^+/HCO_3^- cotransporter enhances NBCe1-mediated HCO_3^- influx in the rat heart. Am J Physiol Cell Physiol. 2012;303:C69-80.

[23] Chiche J, Ilc K, Laferriere J, Trottier E, Dayan F, Mazure NM, et al. Hypoxia-inducible carbonic anhydrase IX and XII promote tumor cell growth by counteracting acidosis through the regulation of the intracellular pH. Cancer Res. 2009;69:358-68.

[24] McIntyre A, Patiar S, Wigfield S, Li JL, Ledaki I, Turley H, et al. Carbonic anhydrase IX promotes tumor growth and necrosis in vivo and inhibition enhances anti-VEGF therapy. Clin Cancer Res. 2012;18:3100-11.

[25] Ajith TA, Jayakumar TG. Mitochondria-targeted agents: Future perspectives of mitochondrial pharmaceutics in cardiovascular diseases. World J Cardiol. 2014;6:1091-9.

[26] Arechederra RL, Waheed A, Sly WS, Supuran CT, Minteer SD. Effect of sulfonamides as carbonic anhydrase VA and VB inhibitors on mitochondrial metabolic energy conversion. Bioorg Med Chem. 2013;21:1544-8.

[27] Perez NG, Piaggio MR, Ennis IL, Garciarena CD, Morales C, Escudero EM, et al. Phosphodiesterase 5A inhibition induces Na^+/H^+ exchanger blockade and protection against myocardial infarction. Hypertension. 2007;49:1095-103.

[28] Ye J, Yang L, Sethi R, Copps J, Ramjiawan B, Summers R, et al. A new technique of coronary artery ligation: experimental myocardial infarction in rats in vivo with reduced mortality. Mol Cell Biochem. 1997;176:227-33.

[29] Geers C, Gros G. Inhibition properties and inhibition kinetics of an extracellular carbonic anhydrase in perfused skeletal muscle. Respir Physiol. 1984;56:269-87.

[30] Dodgson SJ, Forster RE, 2nd. Carbonic anhydrase activity of intact erythrocytes from seven mammals. J Appl Physiol Respir Environ Exerc Physiol. 1983;55:1292-8.

[31] Sahn DJ, DeMaria A, Kisslo J, Weyman A. Recommendations regarding quantitation in M-mode echocardiography: results of a survey of echocardiographic measurements. Circulation. 1978;58:1072-83.

[32] Zat'ovicova M, Tarabkova K, Svastova E, Gibadulinova A, Mucha V, Jakubickova L, et al. Monoclonal antibodies generated in carbonic anhydrase IX-deficient mice recognize different domains of tumour-associated hypoxia-induced carbonic anhydrase IX. J Immunol Methods. 2003;282:117-34.

[33] Strniskova M, Ravingerova T, Neckar J, Kolar F, Pastorekova S, Barancik M. Changes in the expression and/or activation of regulatory proteins in rat hearts adapted to chronic hypoxia. Gen Physiol Biophys. 2006;25:25-41.

[34] Holotnakova T, Ziegelhoffer A, Ohradanova A, Hulikova A, Novakova M, Kopacek J, et al. Induction of carbonic anhydrase IX by hypoxia and chemical disruption of oxygen sensing in rat fibroblasts and cardiomyocytes. Pflugers Arch. 2008;456:323-37.

[35] Raftery EB. Haemodynamic effects of diuretics in heart failure. Br Heart J. 1994;72:S44-7.

[36] Relman AS, Leaf A, Schwartz WB. Oral administration of a potent carbonic anhydrase inhibitor (Diamox). II. Its use as a diuretic in patients with severe congestive heart failure. N Engl J Med. 1954;250:800-4.

[37] Swenson ER. New insights into carbonic anhydrase inhibition, vasodilation, and treatment of hypertensive-related diseases. Curr Hypertens Rep. 2014;16:467.

[38] Swenson ER. Carbonic anhydrase and the heart. Cardiologia. 1997;42:453-62.

[39] van Heerebeek L, Borbely A, Niessen HW, Bronzwaer JG, van der Velden J, Stienen GJ, et al. Myocardial structure and function differ in systolic and diastolic heart failure. Circulation. 2006;113:1966-73.

[40] Gandhi MS, Kamalov G, Shahbaz AU, Bhattacharya SK, Ahokas RA, Sun Y, et al. Cellular and molecular pathways to myocardial necrosis and replacement fibrosis. Heart Fail Rev. 2011;16:23-34.

[41] Vargas LA, Alvarez BV. Carbonic anhydrase XIV in the normal and hypertrophic myocardium. J Mol Cell Cardiol. 2012;52:741-52.

[42] Vargas LA, Diaz RG, Swenson ER, Perez NG, Alvarez BV. Inhibition of carbonic anhydrase prevents the Na^+/H^+ exchanger 1-dependent slow force response to rat myocardial stretch. Am J Physiol Heart Circ Physiol. 2013;305:H228-37.

[43] Bodempudi V, Hergert P, Smith K, Xia H, Herrera J, Peterson M, et al. miR-210 promotes IPF fibroblast proliferation in response to hypoxia. Am J Physiol Lung Cell Mol Physiol. 2014;307:L283-94.

[44] De Giusti VC, Orlowski A, Villa-Abrille MC, de Cingolani GE, Casey JR, Alvarez BV, et al. Antibodies against the cardiac sodium/bicarbonate co-transporter (NBCe1) as pharmacological tools. Br J Pharmacol. 2011;164:1976-89.

[45] Sowah D, Brown BF, Quon A, Alvarez BV, Casey JR. Resistance to cardiomyocyte hypertrophy in ae3-/- mice, deficient in the AE3 Cl-/HCO3- exchanger. BMC Cardiovasc Disord. 2014;14:89.

[46] Cingolani HE, Ennis IL. Sodium-hydrogen exchanger, cardiac overload, and myocardial hypertrophy. Circulation. 2007;115:1090-100.

[47] Garciarena CD, Youm JB, Swietach P, Vaughan-Jones RD. H^+-activated Na^+ influx in the ventricular myocyte couples Ca^{2+}-signalling to intracellular pH. J Mol Cell Cardiol. 2013;61:51-9.

[48] Fliegel L, Karmazyn M. The cardiac Na^+-H^+ exchanger: a key downstream mediator for the cellular hypertrophic effects of paracrine, autocrine and hormonal factors. Biochem Cell Biol. 2004;82:626-35.

[49] Kusumoto K, Haist JV, Karmazyn M. Na^+/H^+ exchange inhibition reduces hypertrophy and heart failure after myocardial infarction in rats. Am J Physiol Heart Circ Physiol. 2001;280:H738-45.

[50] Rentero N, Bruandet N, Milne B, Quintin L. Catechol activation in rat rostral ventrolateral medulla after systemic isocapnic metabolic acidosis. Am J Physiol. 1998;275:R350-6.

[51] Levick SP, Murray DB, Janicki JS, Brower GL. Sympathetic nervous system modulation of inflammation and remodeling in the hypertensive heart. Hypertension. 2010;55:270-6.

Figure Legends

Figure 1. Myocardial infarction in untreated rats induced by coronary artery ligation

Histological analysis of rat heart sections and echocardiographic measurements 3 weeks after myocardial infarction, in rats. **A,** Magnified image of left ventricle stained with Masson´s trichrome. **B,** Percentage of infarct area in the whole left ventricular area. **C,** Wall thickness of infarct area. **D**, Left ventricular endocardial fractional shortening measured in CAL rats, before and 3 weeks after procedure. Data are presented as mean ± SEM. **P* < 0.05, n = 4. Scale bar = 1 mm.

Figure 2. Effect of carbonic anhydrase inhibition on left ventricular chamber dimensions after coronary artery ligation in the rat heart

Myocardial infarction was produced in rats by CAL and maintained for a total of 36 weeks. A group of non-infarcted rats were maintained for 36 weeks and used as control. At 32 weeks, CAL rats were kept up to additional 4 weeks without treatment, or were treated with the CA inhibitor, 6-ethoxzolamide (ETZ), or treated with the CA inhibitor, benzolamide (BZ). **A,** Representative echocardiograms obtained at the end of the experimental protocol in control, CAL, CAL + ETZ, and CAL + BZ rats. Overall results of the left ventricular end systolic (**B**) and left ventricular end diastolic (**C**) dimensions determined in control, CAL, CAL + ETZ, and CAL + BZ rats, before (32 weeks) and after treatments (36 weeks). **P* < 0.05 vs. control; **P < 0.05 vs. CAL. Values are mean ± S.E.M. Brackets on top of bar indicate number of animals analyzed. LVDD, left ventricular diastolic dimension; LVSD, left ventricular systolic dimension; IVSDTh, interventricular diastolic thickness; IVSSTh, interventricular systolic thickness; PWDTh, posterior wall diastolic thickness; PWSTh, posterior wall systolic thickness.

Figure 3. Effect of carbonic anhydrase inhibition on lung fluid content after coronary artery ligation in the rat heart

Bar graph of the effect of ETZ and BZ on dry lung weight/body weight, after 4 week of treatment in MI and control rats. *P < 0.05 vs. control. Values are mean ± S.E.M. Brackets on top of bar indicate number of animals analyzed.

Figure 4. Effect of carbonic anhydrase inhibition on left ventricular function after coronary artery ligation in the rat heart

Left ventricular function measured by echocardiogram in control and CAL rats, before and after CA inhibition treatment. **A**, Left ventricular midwall shortening measured in control, CAL, CAL + ETZ, and CAL + BZ rats, before (32 weeks) and after treatments (36 weeks). **B**, Summary of percentage of midwall shortening relative to control, measured after treatments (36 weeks). **C**, Left ventricular endocardial fractional shortening measured in control, CAL, CAL + ETZ, and CAL + BZ rats, before (32 weeks) and after treatments (36 weeks), as indicated. **D**, Summary of percentage of left ventricular endocardial fractional shortening relative to control, measured after treatments. *P < 0.05 vs. control. $^{**}P$ < 0.05 vs. CAL. Values are mean ± S.E.M. Values in parentheses on top of bars indicate number of animals analyzed.

Figure 5. Effect of the carbonic anhydrase inhibitors 6-ethoxzolamide and benzolamide on collagen deposition after sustained coronary artery ligation in the rat left ventricle

A, Representative left ventricle sections stained with Masson's trichrome viewed at a magnification of 40x, 200x, and 400x, from control (a-c), CAL (d-f), CAL + ETZ (g-i), and CAL + BZ (j-l) rat hearts. The fibrotic area is stained in blue and the viable area red. **E**, Collagen deposition was quantified by automated image analysis and expressed as percentage of tissue

area. Values are mean ± S.E.M; n= 5-15 images, corresponding to 3 different hearts for each group. *$P < 0.05$ vs. control; **$P < 0.05$ vs. CAL.

Figure 6. Effect of 6-ethoxzolamide on carbonic anhydrases IX and VB protein levels and effect of benzolamide on carbonic anhydrase IX protein level, after sustained coronary artery ligation

A, Whole heart lysates were prepared from rat hearts, which were controls, CAL, CAL treated with 6-ethoxyzolamide (ETZ), or CAL treated with benzolamide (BZ). Immunoblots of the heart lysates were probed with antibody against CAIX (*top*), CAVB (*bottom*) and GAPDH (*top and bottom*), as indicated. **B**, Summary of the expression level of CAIX, normalized to GAPDH and quantified by densitometry. **C**, Summary of the expression level of CAVB, normalized to GAPDH and quantified by densitometry. Values are mean ± S.E.M., n = 3. *$P < 0.05$, compared to control. Arrow head indicates position of proteins.

Figure 7. Proposed model of the possible effect of carbonic anhydrase inhibitors on combined action of NHE1 Na^+/H^+ exchanger and carbonic anhydrase in promoting cardiac hypertrophic and heart failure

Adrenergic stimuli, pro-hypertrophic factors, cardiac muscle over-stretch, and MI, linked hyperactivity of the Na^+/H^+ exchanger NHE1 and subsequent Ca^{2+} overload to cardiac hypertrophy [46]. Some of the same factors promote increased CA expression with concomitant Ca^{2+} disturbance as observed in experimental models [8, 19], and in human hypertrophic and failing hearts [9]. Inhibition of CA would slow the rate and magnitude (red arrow) at which the membrane NHE1 alkalinizes the cell. In this context, increased NHE1 activity would lead to an increase in the cytosolic Na^+, which activates Ca^{2+} signaling *via* cytosolic Ca^{2+} rise through the Na^+/Ca^{2+} exchanger (NCX) [47], and initiates hypertrophy [48, 49]. Thus, CA inhibitors may be

therapeutic in limiting catecholamine-driven remodeling and pathologic hypertrophy, as well as ischemia reperfusion damaged and metabolically linked diabetic cardiomyopathy, two major causes of heart failure development [8, 19].

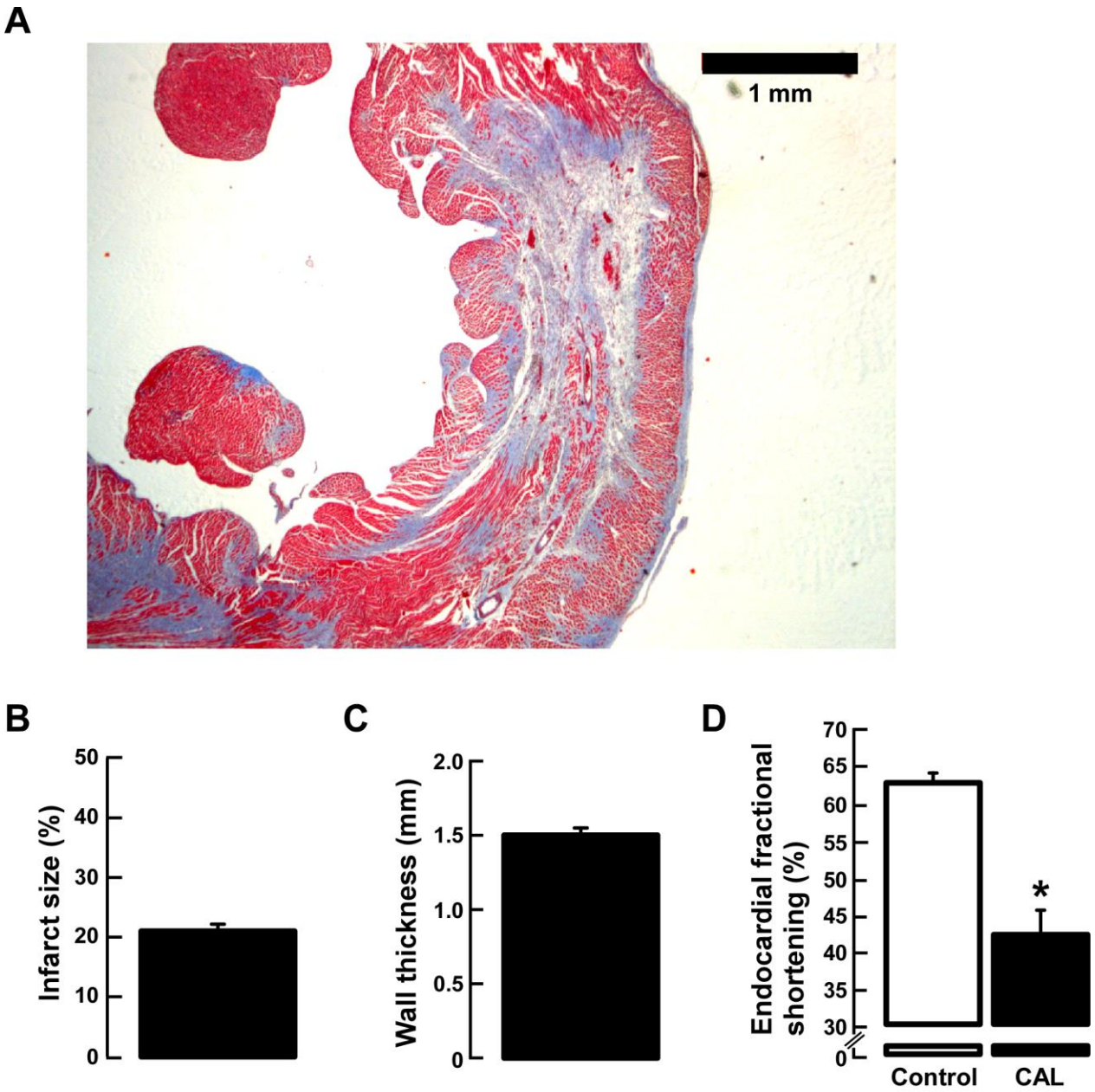

Figure 1

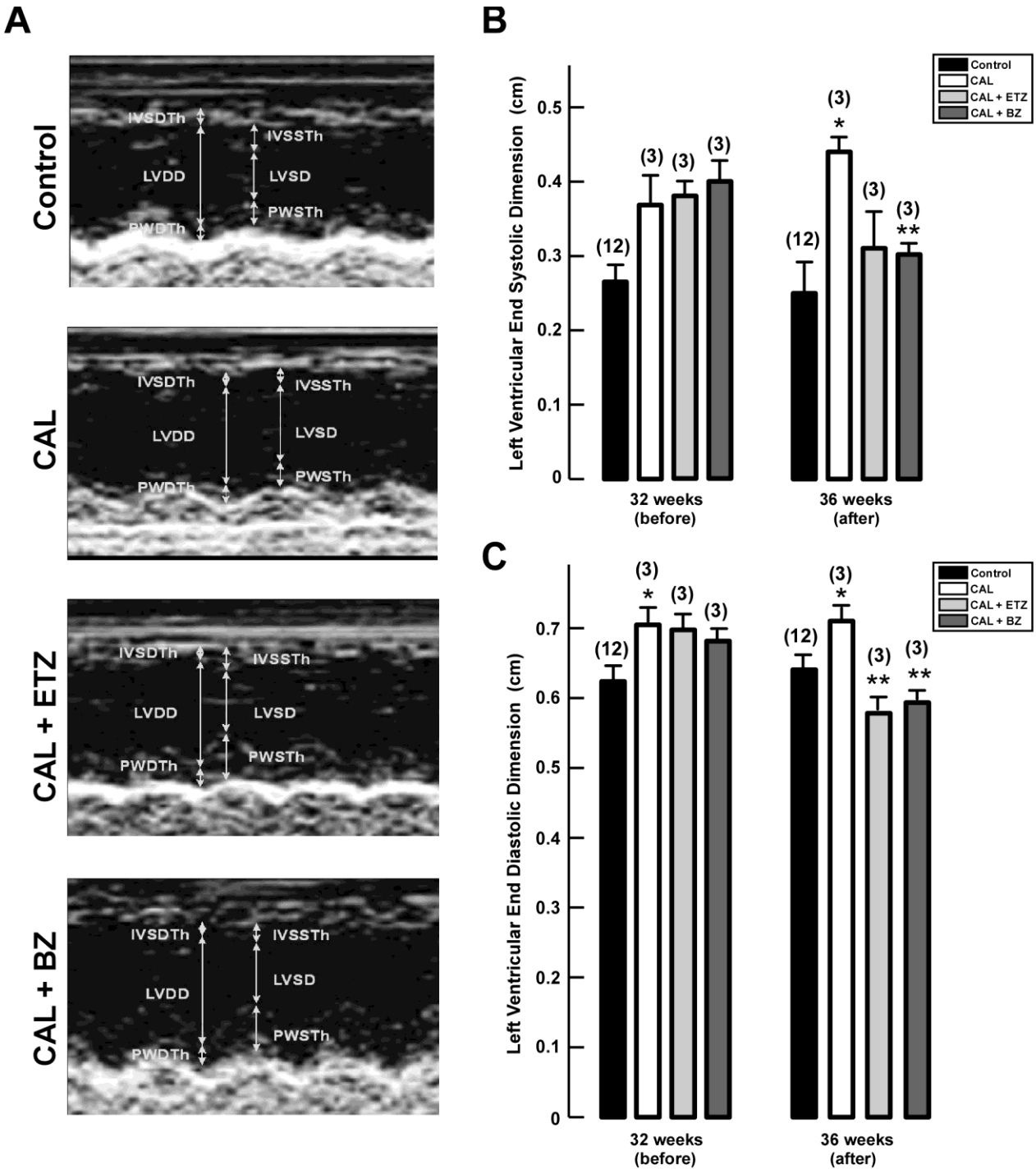

Figure 2

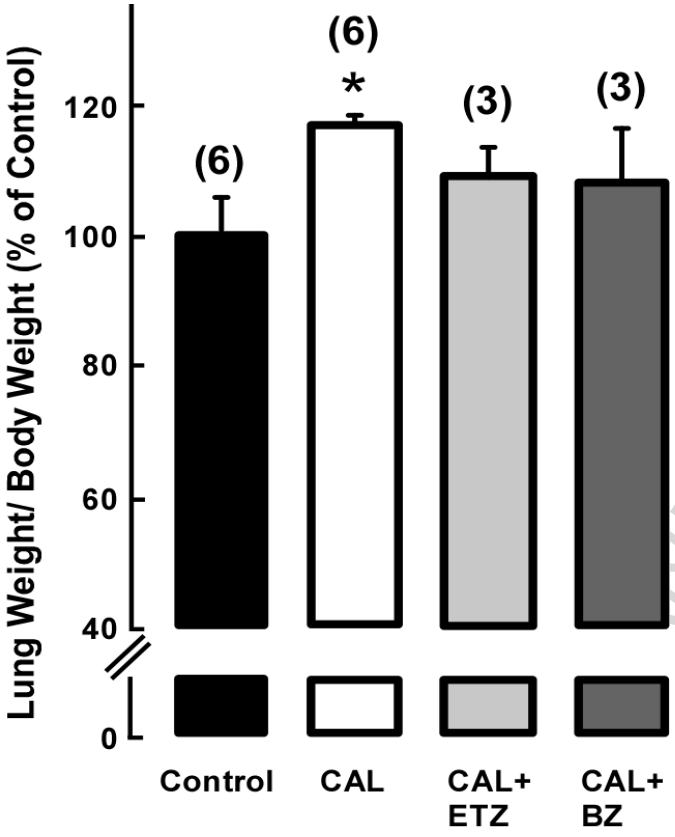

Figure 3

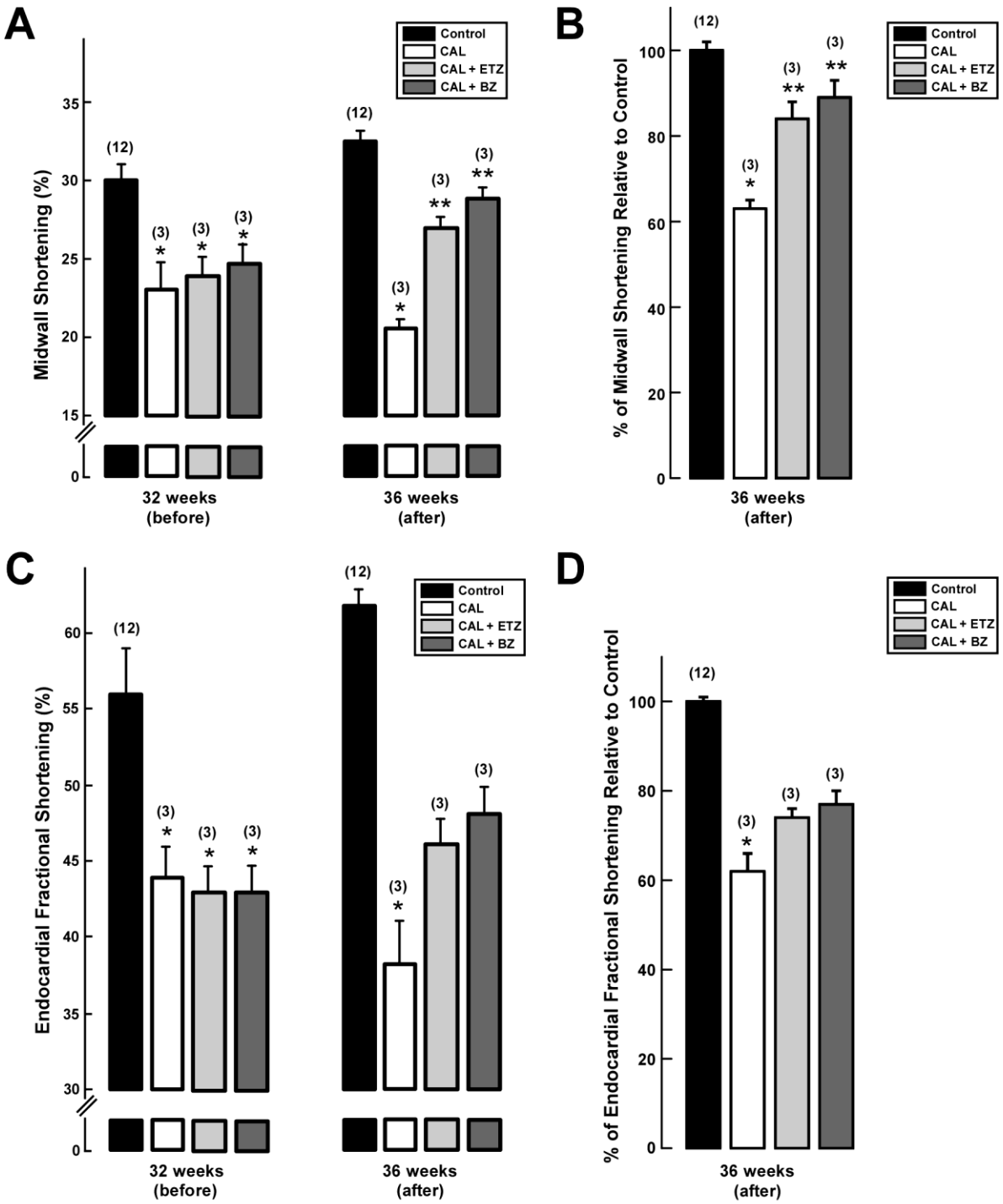

Figure 4

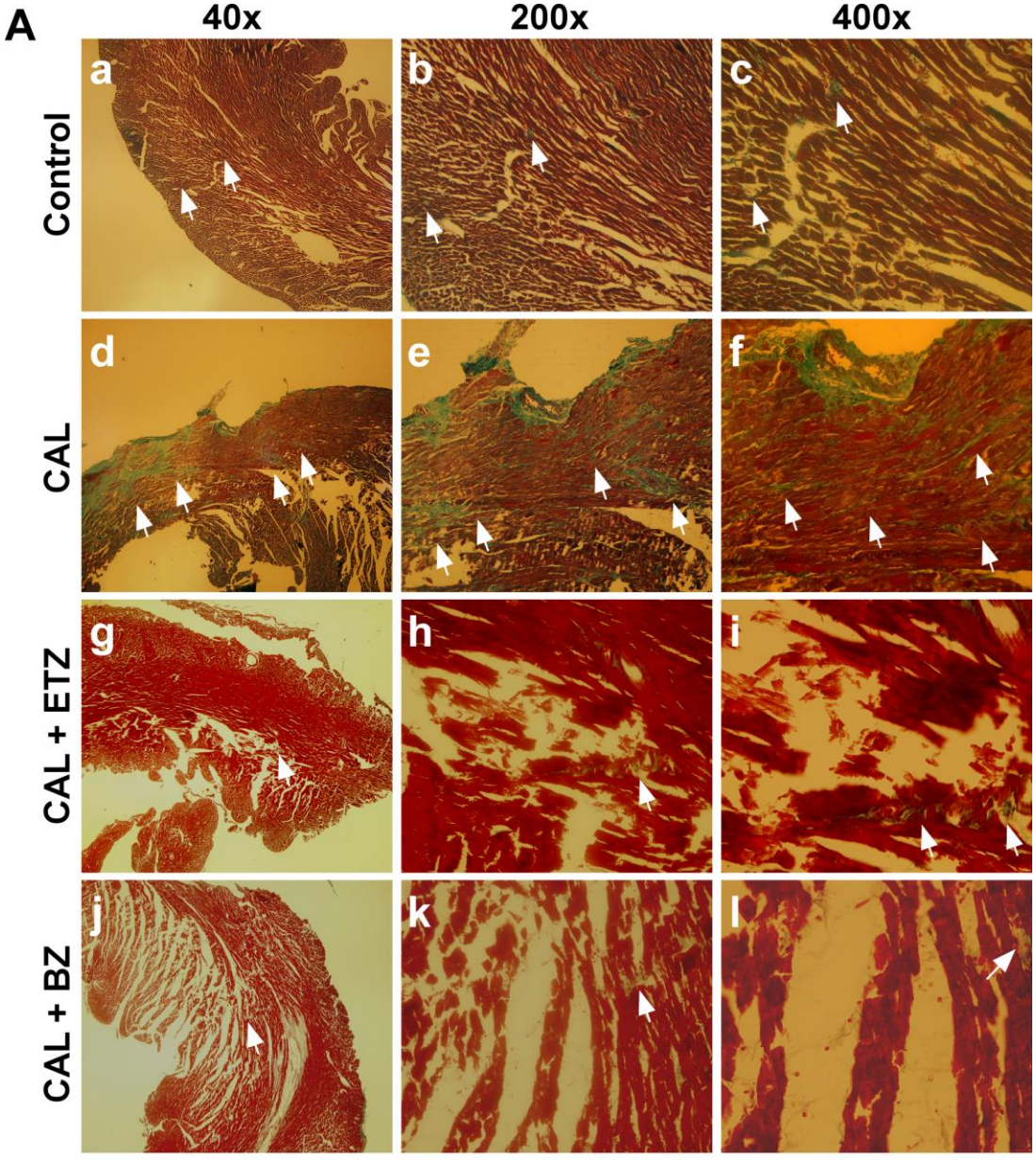

Figure 5

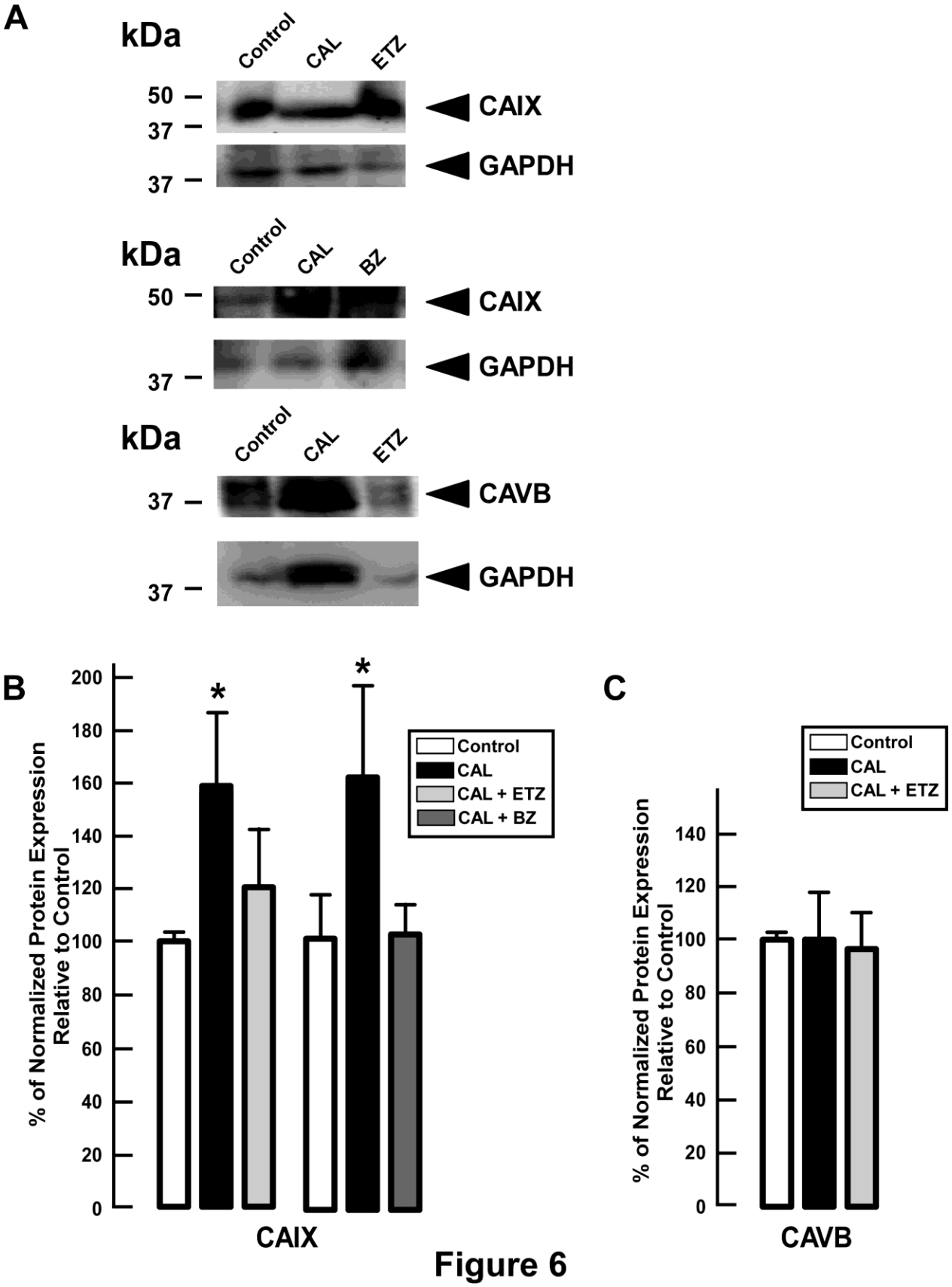

Figure 6

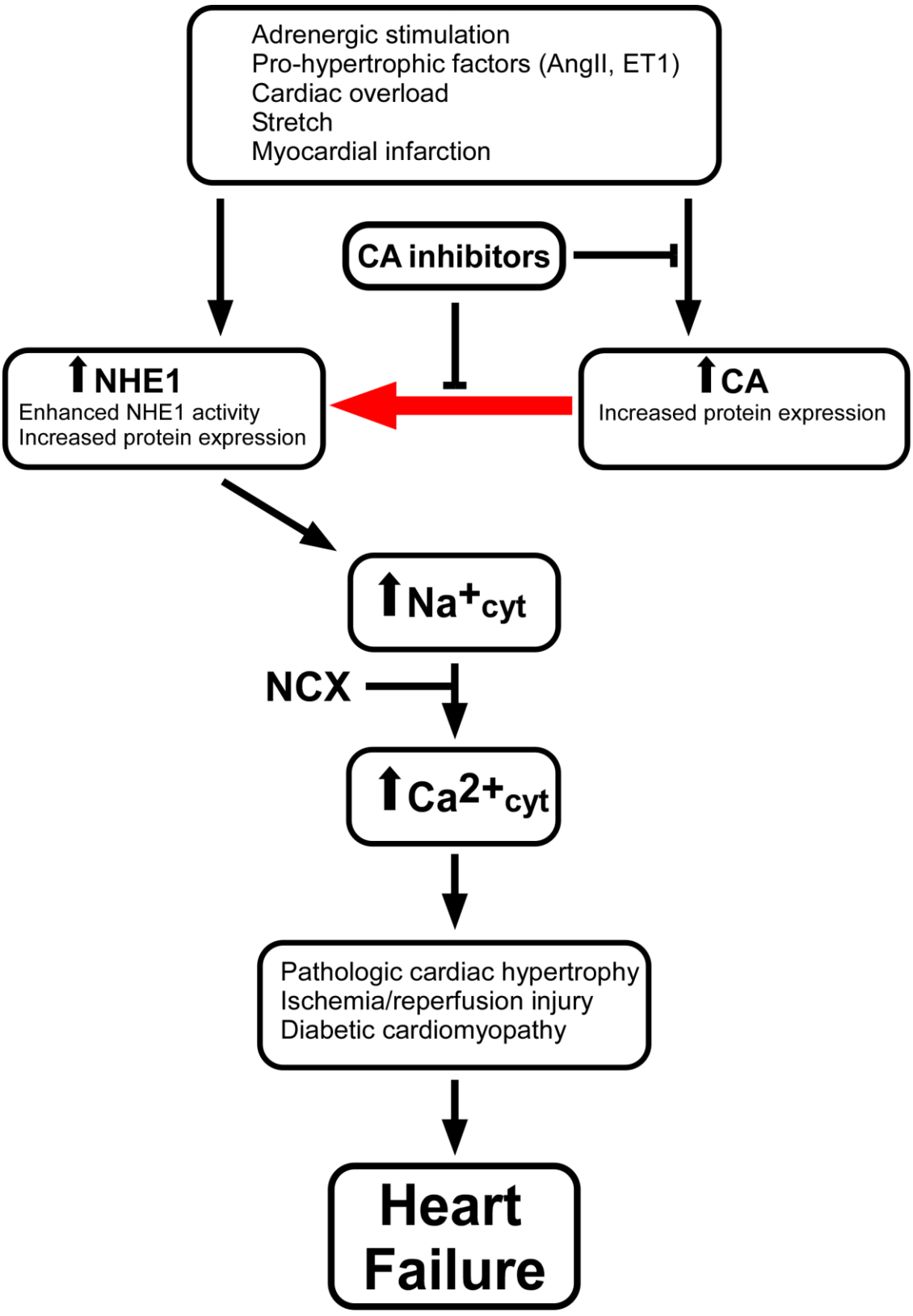

Figure 7

Table 1. Experimental design – Three month-old Wistar rats

Number of animals	Experimental procedure	Treatment	Length of study	Studies performed/ analysis
24	None	None	36 weeks	Echo – week 1 Echo – week 36
12	None	None	36 weeks	Echo – week 32 Echo – week 36 Histology Pathology Immunoblotting (WB)
4	CAL	None	3 weeks	Echo – week 1 Echo – week 3 Histology Pathology
3	CAL	None	36 weeks	Pathology
3	CAL	None	36 weeks	Echo – week 32 Echo – week 36 Histology Pathology Immunoblotting (WB)
3	CAL	ETZ	36 weeks	Echo – week 32 Echo – week 36 Histology Pathology Immunoblotting (WB)
3	CAL	BZ	36 weeks	Echo – week 32 Echo – week 36 Histology Pathology Immunoblotting (WB)

CAL, ligation of the left anterior descending coronary artery; ETZ, 6-Ethoxy-1, 3 benzothiazole-2-sulfonamide; BZ, 5-(benzenesulfonamido)-1, 3, 4-thiadiazole 2 sulfonamide; Echo, echocardiographic examination; WB, Western Blot

Table 2. Baseline cardiac parameters 32 weeks after coronary artery ligation but before initiation of treatment

Cardiac parameter	Control Group (n=12)	Infarct/Untreated Group (n= 12)	Infarct/Carbonic anhydrase inhibitors Group (n= 6)
LVDD (mm)	6.15±0.15	6.35±0.17	6.26±0.28
LVSD (mm)	2.81±0.16	3.60±0.18*	3.51±0.30*
IVSDTh (mm)	1.62±0.03	1.53±0.08	1.50±0.10
IVSSTh (mm)	2.36±0.17	1.77±0.10*	1.73±0.10*
PWDTh (mm)	1.67±0.04	1.74±0.06	1.68±0.06
PWSTh (mm)	2.93±0.07	2.86±0.09	2.67±0.09*

LVDD, left ventricular diastolic diameter; LVSD, left ventricular systolic diameter; IVSDTh, interventricular diastolic thickness; IVSSTh, interventricular systolic thickness; PWDTh, posterior wall diastolic thickness; PWSTh, posterior wall systolic thickness; $P < 0.05$ vs. control group; Values are mean ± SEM.

Table 3. Body weight in control and infarcted rats, after coronary artery ligation and before (32 weeks) and after treatments (36 weeks)

	Control Group n = 6		Infarct Group n = 6		Infarct/ETZ Treated Group n = 3		Infarct/BZ Treated Group n = 3	
	Before	**After**	**Before**	**After**	**Before**	**After**	**Before**	**After**
Body weight (g)	499±9	489±16	520±11	523±14	535±19	547±38	509±9	494±16

n = number of animals; Values are mean ± SEM.

Funding

This work was funded by a Grant from Agencia Nacional de Promoción Científica y Tecnológica to BVA (FONCyT, PICT2013 N° 1976). LAV was a recipient of a felloship from Consejo Nacional de Investigaciones Científicas y Técnicas (CONICET, Type II Postdoctoral Felloship).

Highlights

♦ In heart failure rats after prolonged myocardial infarction, carbonic anhydrase inhibition (CAI) by benzolamide (BZ) and ethoxzolamide (ETZ) improves cardiac function.

♦ The potent CA inhibitors BZ and ETZ limit interstitial fibrosis and prevent heart remodeling, in heart failing rats.

♦ Inhibition of membrane-bound CAIX isozyme appears to be the critical site of CAI in the reduction of post infarction cardiac dysfunction and fibrotic remodeling.